



ATS11-03325

Tunnel Face Stability Analysis in Soft Ground in Urban Tunneling by EPB Shield (Case Study : 7th Line in Tehran Metro)

J. Mohammadi*, K. Shahriar, P. Moarefvand***, S.Hosseini***

*Department of Mining Engineering, Islamic Azad University Tehran South Branch, Iran, Email : jamohammadi1982@yahoo.com

**Department of Mining, Metallurgy and Petroleum Engineering, Amirkabir University of Technology, Hafez 424, Tehran 15875-4413, Iran, Email: k.shahriar@aut.ac.ir

*** Department of Mining, Metallurgy and Petroleum Engineering, Amirkabir University of Technology, Hafez 424, Tehran 15875-4413, Iran, Email: parvizz@aut.ac.ir

ABSTRACT

Traffic congestion and environmental factors are creating a demand for greater utilization of underground spaces in urban areas. In mechanized excavation of subway tunnels, the Earth Pressure Balanced Shield (EPBS) has been developed in the recent decades for managing the instability of the excavation profile in complicated geotechnical conditions in urban areas. During the advancement of an EPBS, the face-stabilizing pressure is one of the most important factors of critical and principle to be evaluated correctly. In tunneling by EPBS, high face pressure often leads to surface upheaval whereas low face pressure leads to sudden collapse of the face and ultimately settlement of the surface. Both of these misevaluated pressures may cause the damages which followed by pert of time and finance. This paper is discussed about urban tunneling by EPBS in soft ground conditions and focused on calculation of face-stabilizing pressure applying to the case of 7th line in Tehran metro project. Face-support pressure is estimated by most current methods of limiting equilibrium analysis and limiting analysis in excavated parts (two stations) of direction with different and difficult geotechnical conditions. Obtained results compared to EPBS operational results which showed the results of Broere analytical method is most attractive and realistic among others. For one of the excavated stations calculated value of the Broere analytical method obtained 78.406 KPa and EPBS actual value was equal to 81.01 KPa. Due to results verification that illustrate a good adjustment with the actual values, quantity face-stabilizing pressure is predicted for some of the alignment unexcavated stations (S7, V7, W7 and X7) which can be used in built procedure. Maximum value was quantity 246.351 KPa for station V7 and minimum value obtained quantity 25.866 KPa for station W7.

KEYWORDS

Tunneling, face-stabilizing pressure, EPBS, analytical method, 7th line of Tehran metro.

INTRODUCTION

As excavation of tunnels in unfavorable geotechnical conditions and in heavily populated urban environments is becoming prevalent, the importance of maintaining tunnel face stability is reaching more importance. Ensuring tunnel face stability is directly related to the safe and successful construction of a tunnel. In this context, tunnel face stability analysis directly relates to face-support pressure. The correct evaluating of face pressure to avoid face instability depends on various factors, such as cohesion, friction angle and permeability of the ground, type of the machine, advance rate, unit weight of

slurry or conditioned soil, tunnel diameter, overburden, and location of the ground water table. Many researchers have proposed analytical approaches to determine the required pressure to stabilize the tunnel face. Most of them are based either on limiting equilibrium analysis (Broms and Bennmark, 1967; Krause, 1987; Jancsecz and Steiner, 1994;

Anagnostou and Kovári, 1996; Broere, 2001; Carranza-Torres, 2004), or limiting analysis (Atkinson and Potts, 1977; Davis et al., 1980; Leca and Dormieux, 1990).

In the first part of the paper, some referenced methods for evaluating the stability of face are presented then project characteristics are described. In the next part face-stabilizing pressure is calculated in two excavated stations of 7th line of

Tehran subway (stations N7 & O7) by limiting equilibrium analysis and limiting analysis methods. Then obtained results are compared to face-stabilizing pressures of EPBS operational. In fact, purpose of this comparison is the selection of the best analytical method for the project. Finally as logical consequence, suitable method is selected among others, and is predicted face-support pressure in unexcavated various parts (stations S7, V7, W7 and X7).

2. Limiting Equilibrium and Limiting Analysis Methods (LEM & LAM)

2.1 Method of Broms and Bennemark (1967)

A well solution based on Tresca material is [Broms and Bennemark's solution](#). They suggested the stability ratio N (Eq. (1)) for a vertical opening. This solution is independent of the overburden-to-diameter ratio.

$$N = (q_s - \sigma_T) / c_u + (C + R) \cdot Y / c_u \quad (1)$$

Where Y = the total unit weight of the ground, c_u = undrained shear strength of the ground, q_s = surcharge, R = radius, σ_T = the minimum face support pressure and C = overburden (cover depth).

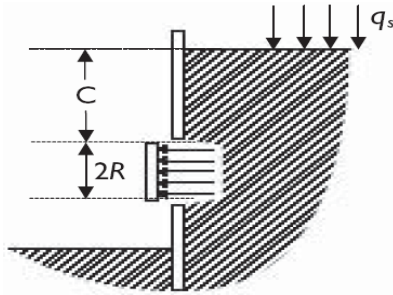


Figure 1. The tunnel-face stability model of the method of Broms & Bennemark.

Empirically, the instability conditions are associated with a value of $N \geq 6$. Therefore, the face-stabilizing pressure σ_T is:

$$\sigma_T = Y \cdot (C + R) + q_s - N \cdot c_u \quad (2)$$

where $N = 6$.

2.2 Method of Atkinson and Potts (1977)

Plastic limit analysis approaches employ a plane strain condition. [Atkinson and Potts](#) investigated the required support pressure for an unlined tunnel cross section away from tunnel heading in a cohesionless soil. The minimum support pressure (σ_T) is :

$$\sigma_T = 2k_p YR / (k_p^2 - 1) \quad (3)$$

where $k_p = (1 + \sin \phi) / (1 - \sin \phi)$ and ϕ = the soil friction angle.

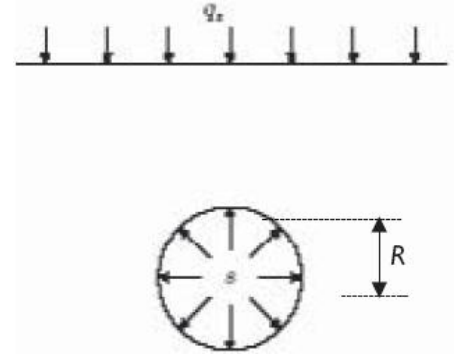


Figure 2. The tunnel-face stability model of the method of Atkinson & Potts.

2.3 Method of Davis et al. (1980)

Like previous solution, this method employs a plane strain condition too. [Davis et al.](#) investigated face-stabilizing pressure for purely cohesive material. This method allows the stability analysis of a tunnel with radius R , in a cohesive soil, where a rigid support is installed at a distance P from the face. Hence these researchers presented distance P (Fig.3) and the stability ratio N . The stability ratio in the two cases of cylindrical (Eq.(4)) and spherical (Eq.(5)) is calculated.

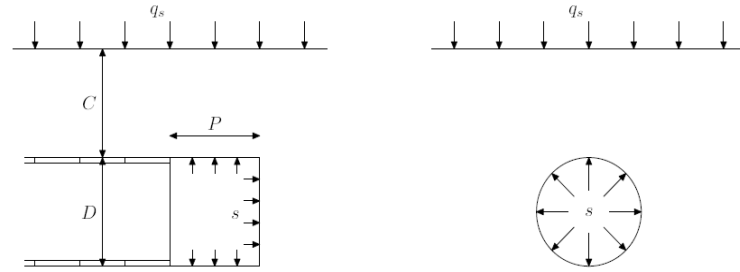


Figure 3. The loading schemes of the method of Davis et al.

$$N = 2 + 2 \ln(C/R + 1) \quad (4)$$

$$N = 4 + 2 \ln 9C/R + 1 \quad (5)$$

2.4 Method of Krause (1987)

The minimal support pressures needed for a semi-circular and spherical limiting equilibrium mechanism which have been calculated by [Krause](#) in a limiting equilibrium analysis using the shear stresses on the sliding planes. Of the three mechanisms proposed, the quarter circle (Fig.4b) will always yield the highest minimal support pressure:

$$\sigma_T = (DY/3 - \pi c/2) / \tan \phi \quad (6)$$

As [Krause](#) already indicates this may not always be a realistic representation of the actual failure body. In many cases the half-spherical body (Fig.4c) will be a better representation. In that case the minimal support pressure can be found from:

$$\sigma_T = (DY/9 - \pi c/2) / \tan \phi \quad (7)$$

where D = tunnel diameter and c = soil cohesion.

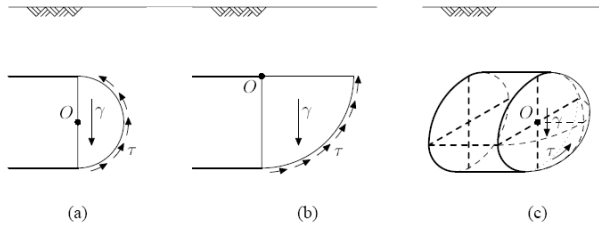


Figure 4. Circular and spherical failure mechanisms

2.5 Method of Leca and Dormieux (1990)

The purpose of limiting analysis is to provide an estimate of stability conditions for a mechanical system regardless of the behaviour of the material. Leca and Dormieux used the limiting analysis concept to evaluate the stability of a tunnel face driven in frictional soil and compared these results with centrifuge tests performed by Chambon and Corte (1994). A reasonable agreement was found between the theoretical upper bound estimates and the face pressures measured at failure from the tests. Therefore, by modifying the upper bound solution suggested by Leca and Dormieux the three-dimensional analytical model. Three failure mechanisms have been considered. They all involve the movement of solid conical blocks with circular cross-sections. The opening of each cone is equal to $2\phi'$ and its velocity V is parallel to its axis (Fig.5).

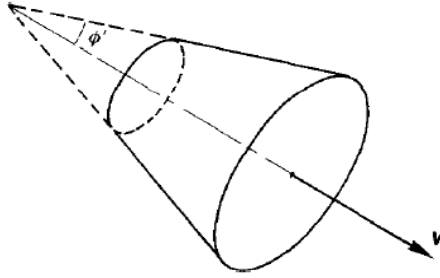


Figure 5. Conical blocks and kinematic conditions used in M1 and M2

Therefore condition is satisfied along the failure surfaces between the moving blocks and the rest of the ground.

The two mechanisms M1 and M2 are shown in the Fig.6 and Fig.7 respectively. M1 is a collapse mechanism, whereas M2 refers to blow out failure. Failure is due to the collapse of one conical block in M1.

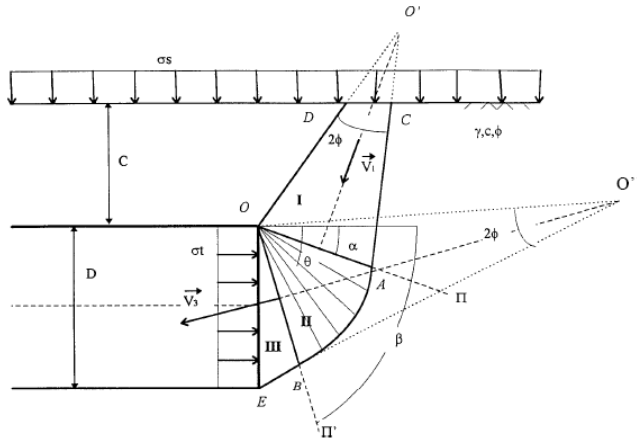


Figure 6. Failure Mechanism M1 (Collapse)

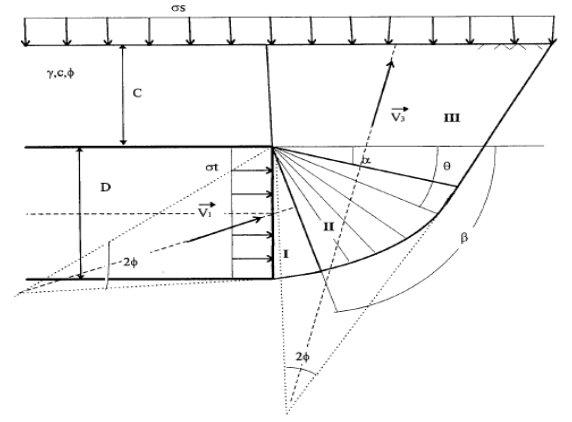


Figure 7. Failure mechanism M2 (upheaval)

Leca and Dormieux obtained face-support pressure (σ_T) for upper bound :

$$\sigma_T = N_S q_s + N_Y DY \quad (8)$$

where q_s =surcharge, D =diameter, Y =unit weight of ground and N_S and N_Y are non dimensional weighting coefficients.

$$N_S = \frac{1}{\cos \alpha \cos^2 \phi} \frac{\sin(\beta - \phi) R_E^2}{\sin(\beta + \phi) R_A} \quad (9)$$

$$N_Y = \frac{1}{3} \left[\tan \alpha R_B + \frac{\cos \phi \cos(\beta + \phi) R_C^3}{2 \sin \phi \sin(\beta + \phi) R_A} - \frac{1}{2 \sin \phi \cos \alpha \cos^2 \phi} \frac{\sin(\beta - \phi) R_E^3}{\sin(\beta + \phi) R_A} \right] \quad (10)$$

$$R_A = \frac{\sqrt{\cos(\alpha - \phi) \cos(\alpha + \phi)}}{\cos \phi} \quad (11)$$

$$R_B = \frac{\cos(\alpha - \phi) \cos(\alpha + \phi)}{\sin 2\phi} \quad (12)$$

$$R_C = \frac{\cos(\alpha + \phi)}{\cos \phi} \left[\frac{\sin(\beta - \phi)}{\sin(\beta + \phi)} \right]^{1/2} \quad (13)$$

$$R_D = \frac{\sin \beta}{\sin \phi \sin(\beta + \phi)} \quad (14)$$

$$R_E = \frac{\sin(\beta - \phi) \cos(\alpha + \phi)}{\sin(\beta + \phi)} \quad (15)$$

$$\alpha = 49 - \phi/2 \quad (16)$$

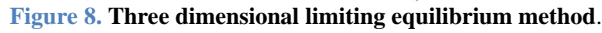
$$\beta = \pi/4 + \alpha/2 \quad (17)$$

where R_A , R_B , R_C , R_D and R_E are non dimensional factors, ϕ =friction angle of the soil, α =angle of sliding plane, and β =failure angle(slip angle).

Note: N_S is almost always smaller than N_Y and is equal to zero for value of ϕ when $C/D \geq 0.6$.

2.6 Method of Jancsecz and Steiner (1994)

So you see the Fig.8, that shows the three dimensional failure scheme that consists of a soil wedge (lower part) and a soil silo (upper part). Jancsecz and Steiner investigated the effects of soil arching above the tunnel heading, and suggested a three-dimensional earth pressure coefficient K_{A3} in the Table 2


$$\sigma_T = 4E/\pi D^2 \quad (18)$$

$$\sigma_T = 4E/\pi D^2 \quad (18)$$

$$E = -\frac{(\cos \beta . \tan \varphi - \sin \beta) . \Sigma(G_s + G_w) + \Sigma(2T + K)}{\sin \beta . \tan \varphi + \cos \beta} \quad (19)$$
$$G_s = B.D.\cot \beta.\sigma'_v \quad (20)$$

$$G_w = \frac{B.D^2.\gamma'.\cot \beta}{2} \quad (21)$$

$$T = \frac{D^2 \cdot \cot \beta}{2} (c + K_y \cdot \bar{\sigma}'_v \cdot \tan \varphi) \quad (22)$$

$$K = \frac{B.D.c}{\sin \beta} \quad (23)$$

Table 1. Variation of slip angle

The vertical pressure is calculated according to [Terzaghi's solution](#), so that in dry soil conditions (Eq.(22)) and when there is underground water (Eq.(23)).

$$\sigma'_V = \frac{a\gamma' - c}{k \cdot \tan \varphi} \left[1 - e^{\frac{-H}{a} \cdot K \cdot \tan \varphi} \right] + \sigma'_{Vd} \cdot e^{\frac{-H}{a} \cdot K \cdot \tan \varphi} \quad (25)$$

$$\sigma'_{vd} = \frac{a\gamma_d - c}{k \cdot \tan \varphi} \left[1 - e^{-\frac{C-H}{a} \cdot K \cdot \tan \varphi} \right] + q_0 \cdot e^{-\frac{C-H}{a} \cdot K \cdot \tan \varphi} \quad (26)$$

$\frac{C}{D}$	K_{A3}				
	φ =20	φ =25	φ =30	φ =35	φ =40
0	0.38 6	0.310	0.24 8	0.19 9	0.15 9
1	0.35 4	0.279	0.22 2	0.17 7	0.14 1
2	0.34 8	0.273	0.21 7	0.17 3	0.13 8
3	0.34 5	0.271	0.21 4	0.17 1	0.13 6

This three-dimensional static system (Fig.9) is based upon the silo theory (Janssen, 1895) and was first applied by Horn (1961) to the investigation of tunnel face stability. The analysis is performed in drained condition, and a difference between the stabilizing water pressure and the effective pressure in the plenum of an EPBS is presented.

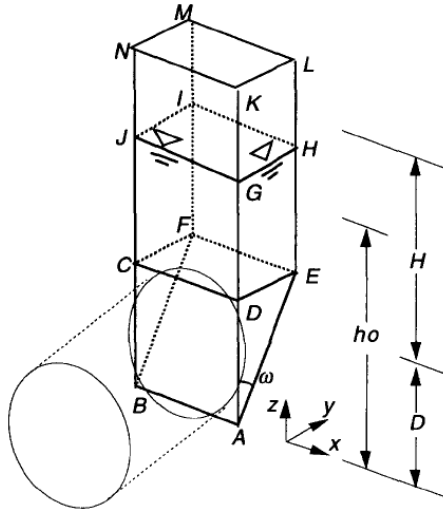


Figure 9. The tunnel-face stability model of the method of Anagnostou & Kovari.

At limiting equilibrium, the effective stabilizing pressure (Eq.(27)) depends on the tunnel diameter D , on the overburden H , on the piezometric head h_F , on the elevation of the water table h_o , on the shear strength parameters c and ϕ , on the submerged unit weight γ (for the soil beneath the water table), and the dry unit weight γ_d (for the soil above the water table).

$$\sigma_T = F_0 \gamma D - F_1 c + F_2 \gamma \Delta h - F_3 c \Delta h / D \quad (27)$$

where F_0 , F_1 , F_2 and F_3 are non dimensional coefficients (Fig.10) and $\Delta h = h_o - h_F$.

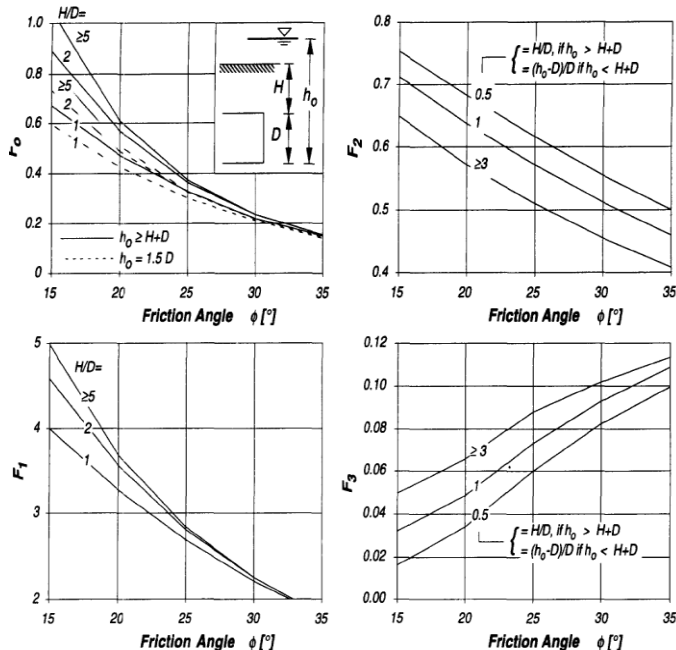


Figure 10. Nomograms for the dimensionless coefficients F_0 to F_3

2.8 Method of Broere (2001)

This method modified some important limitations of the current analytical methods such as the heterogeneity of the ground at the face (Fig.12). Broere method is based wedge and silo theory that some forces are acting on the wedge (Fig.11).

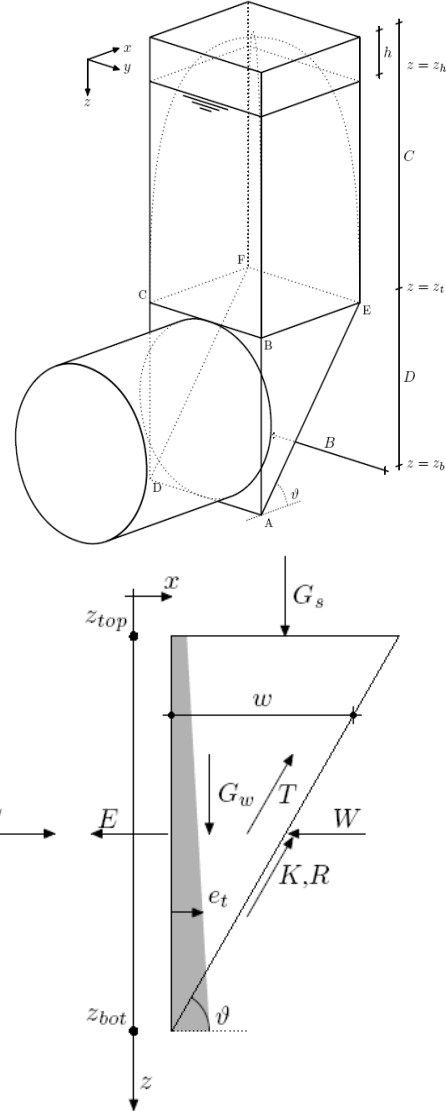


Figure 11. Wedge and silo model(up) and forces acting on the wedge(down) in Broere method.

This wedge is assumed to be a rigid body, loaded its effective weight G_w and the overburden resulting from the soil silo, G_s . On the triangular side planes of the wedge the full cohesive-frictional forces T are taken into account, derived from the horizontal effective stress. The shear force acting on the slanted front plane of the wedge, resulting from the normal force N acting on this plane, is split in two parts. The frictional part R depends only on the angle of internal friction ($R = N \tan \phi$). The force K depends only on the cohesion of the soil or, in an undrained analysis, on the undrained shear strength. Equilibrium of these forces results

in an effective earth force E , which has to be countered by the effective support force S' . This is the difference between the total support force S and the water force W that results from the pore pressure. For a given wedge angle θ the resulting earth force E can be calculated. The minimal support pressure can be found by iterating over the angle θ and maximizing E .

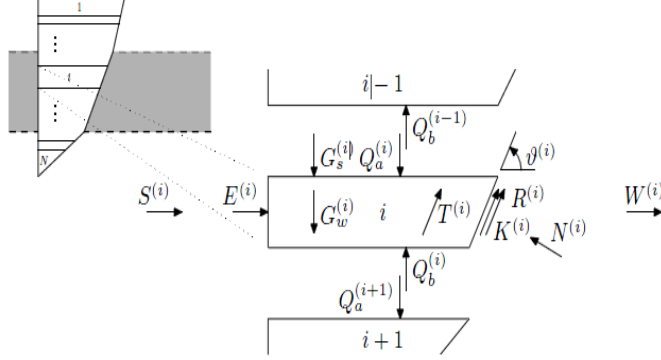


Figure 12. Definition of symbols in the multilayered wedge model

Fig.12 shows the failure wedge is subdivided in N smaller bodies, possibly of different thickness, inside each of which the soil conditions are homogeneous. The soil conditions may vary between these slices, as may the wedge angle $\theta^{(i)}$ between the i 'th slice's slanted failure plane and the horizontal. Each slice i is loaded by the resulting forces from the slice above ($i - 1$) and below ($i + 1$), $Q_a^{(i)}$ and $Q_b^{(i)}$ respectively, the effective weight of the slice itself $G_w^{(i)}$ and an overburden force $G_s^{(i)}$. At the slanted failure plane there is a cohesive force $K^{(i)}$ acting parallel to the plane, as well as a friction force $R^{(i)}$, which results from the normal force $N^{(i)}$, working perpendicular to the failure plane. The side faces of the wedge are each assumed to be loaded by the shear forces $T^{(i)}$, which act in the same direction as $K^{(i)}$, against the deformation direction of the wedge. Force equilibrium will yield the effective earth force $E^{(i)}$ at the face which, combined with the water force $W^{(i)}$, is equal to the support force $S^{(i)}$.

There is vertical and horizontal equilibrium in condition of:

$$E^{(i)} + 2T^{(i)} \cos \theta^{(i)} + (K^{(i)} + R^{(i)}) \cos \theta^{(i)} - N^{(i)} \sin \theta^{(i)} = 0 \quad (28)$$

$$Q_a^{(i)} + G_s^{(i)} + G_w^{(i)} - Q_b^{(i)} - 2T^{(i)} \sin \theta^{(i)} - (K^{(i)} + R^{(i)}) \sin \theta^{(i)} - N^{(i)} \cos \theta^{(i)} = 0 \quad (29)$$

$$R^{(i)} = N^{(i)} \tan \varphi^{(i)} \quad (30)$$

Combination of equations (28) and (29) lead to:

$$G_s^{(i)} + G_w^{(i)} + Q_a^{(i)} - Q_b^{(i)} + 2T^{(i)} \frac{1}{\zeta_-^{(i)}} + K^{(i)} \frac{1}{\zeta_-^{(i)}} + E^{(i)} \frac{\zeta_+^{(i)}}{\zeta_-^{(i)}} = 0 \quad (31)$$

Because of shorthand notation:

$$\zeta_+ = \tan \varphi \sin \theta + \cos \theta \quad (32)$$

$$\zeta_- = \tan \varphi \cos \theta - \sin \theta \quad (33)$$

Each slice has to satisfy the equilibrium as well as the continuity condition:

$$Q_a^{(i)} = Q_b^{(i-1)} \quad (34)$$

Boundary conditions: $Q_b^{(N)} = 0$ and $Q_a^{(1)} = 0$

For slice N:

$$Q_a^{(N)} = Q_b^{(N-1)} = - \left[G_s^{(N)} + G_s^{(N-1)} + G_w^{(N)} + G_w^{(N-1)} + 2T^{(N)} \frac{1}{\zeta_-^{(N)}} + 2T^{(N-1)} \frac{1}{\zeta_-^{(N-1)}} \right] \quad (35)$$

This result can be combined with the equilibrium relation for slice N-1:

$$Q_a^{(N-1)} = Q_b^{(N-2)} = - \left[G_s^{(N)} + G_s^{(N-1)} + G_w^{(N)} + G_w^{(N-1)} + 2T^{(N)} \frac{1}{\zeta_-^{(N)}} + 2T^{(N-1)} \frac{1}{\zeta_-^{(N-1)}} + K^{(N)} \frac{1}{\zeta_-^{(N)}} + K^{(N-1)} \frac{1}{\zeta_-^{(N-1)}} + E^{(N)} \frac{\zeta_+^{(N)}}{\zeta_-^{(N)}} + E^{(N-1)} \frac{\zeta_+^{(N-1)}}{\zeta_-^{(N-1)}} \right] \quad (36)$$

Where,

$$E = - \frac{\zeta'_-}{\zeta'_+} \left[G_s + G_w + \sum_{i=1}^N \frac{1}{\zeta_-^{(i)}} (2T^{(i)} + K^{(i)}) \right] \quad (37)$$

$$S = E + W \quad (38)$$

And so on the above equations, finally minimum face-stabilizing pressure (σ_T) is equal to:

$$\sigma_T = 4S / \pi D^2 \quad (39)$$

2.9 Method of Carranza-Torres (2004)

Carranza-Torres integrated method of Caquot-Kerisel (1956). Carranza's model considers the equilibrium condition for material undergoing failure above the crown of a shallow circular (cylindrical or spherical) cavity. The material has a unit weight γ and a shear strength defined by Mohr-Coulomb parameters c and φ , the cohesion and the friction angle respectively. A support pressure P_s is applied inside the tunnel, while a surcharge q_s acts on the ground surface. For the situation presented in the Fig.13, Carranza's solution defines the value of face-stabilizing pressure (P_s) as the minimum or critical pressure below which the tunnel will collapse:

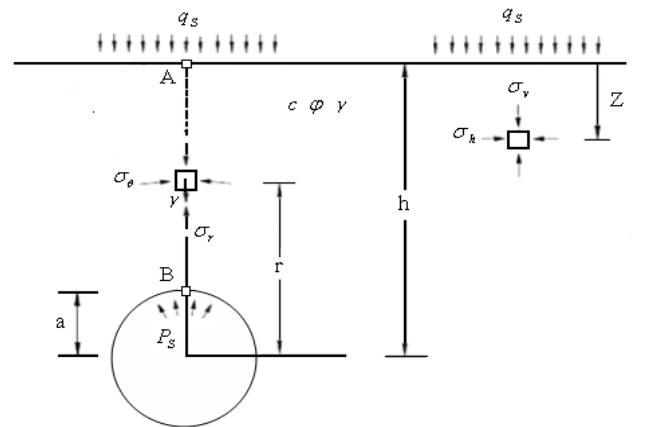


Figure 13. Main design of Caquot-Kerisel

$$\frac{p_s}{\gamma a} = \left[\frac{q_s}{\gamma a} + \frac{c}{\gamma a} \cdot \frac{1}{\tan \varphi} \right] \left[\frac{h}{a} \right]^{-K(N_\varphi^{FS}-1)} - \frac{1}{K(N_\varphi^{FS}-1)-1} \left[\left(\frac{h}{a} \right)^{1-K(N_\varphi^{FS}-1)} \right] - \frac{c}{\gamma a} \frac{1}{\tan \varphi} \quad (40)$$

Where α =the tunnel radius, h =axis depth below the surface, FS =factor of safety(Eq.(42)).

$$N_\varphi^{FS} = \frac{1 + \sin \left(\tan^{-1} \frac{\tan \varphi}{FS} \right)}{1 - \sin \left(\tan^{-1} \frac{\tan \varphi}{FS} \right)} \quad (41)$$

$$FS = \frac{c}{c^{cr}} = \frac{\tan \varphi}{\tan \varphi^{cr}} \quad (42)$$

3. Project characteristics

The Tehran Metro line 7 in Iran has 27 km length and is divided into two parts i.e. North-South Lot and East-West Lot.(Fig.14). 7th line of Tehran metro is consist of 26 stations that North-South Lot has 13 stations and East-West Lot has 13 stations too. The field explorations and surveying were performed by boring 37 boreholes. Distance between boreholes is generally in the range of between 800m and 1150m approximately.



Figure 13. Direction of 7th line of Tehran metro

At first the excavation started in North-South Lot from station N7. There are main data of 7th line of Tehran metro, North-South section in the Table 3.

Table 3. main data of 7th line of Tehran metro

Name of tunnel	7 th line of Tehran metro – North-South section
Purpose/function of the tunnel	Metro line
Total length	14.8 Km
Number of stations	13(N7,O7,P7,Q7,R7,S7,T7,U7,V7,W7,X7,Y7,Z7)
Maximum slope	5.0%
Minimum overburden	9.5 meter to prevent encountering civil limitations
Minimum tunnel crown distance from other metro lines	5.0 meter
Foreseen Construction methods	EPB TBM – 14800 m (100% of total)
Cutterhead diameter	9.16 meter
TBM tunnel typical section	8.15 m internal diameter lined with precast elements

The Tables 4, 5 and 6 show soil classification, chainage, soil category and finally geotechnical data of direction.

Table 4. Soil classification of North-South Lot of Tehran metro line 7

Station	BSCS	Chainage
N7	GML,MLG	11+500-12+500
O7	GWM,GML,MLG	12+500-13+700
P7	GWM,GML,GCI	13+700-14+750
Q7	GCL,GCI,CLG,CIG	14+750-15+300
R7	GML,GCL	15+300-15+800
	GPC,GPM,GWC	15+800-16+500
S7	GPC,GPM,GWC,GWM	16+500-17+200
	GPC,GPM	17+200-17+600
	GWM,GML	17+600-18+000
T7	GWM,GWC,GPC,GML	18+000-18+700
U7	GWM,GML	18+700-19+400
	GCL,GCI,SMI,GWM	20+000-20+900
V7	ML,CL	20+900-21+600
	CL,MIS	21+600-22+200
W7	GCL,CLG,CL	22+200-22+500
	GCL,CLG	22+500-23+700
X7	CLG,CL,GCL,CLG	23+700-24+150
	CL	24+150-24+650
	CLG,CL	25+200-25+550
Y7	GML,CLG	25+550-26+200
Z7	GWC,GPC	26+200-26+600

Table 5. Soil grouping for geotechnical design purpose

Soil Category	Classification Symbols	
	Group	Subgroup
I	G-F S-F	GWM , GPM GWC , GPC SWM , SPM SWC , SPC
II	GF SF	GML , GMI GCL , GCI SML , SMI SCL , SCI
III	FG FS	MLG , MIG CLG , CIG MLS , MIS CLS , CIS
IV	F	ML , MI CL , CI

Table 6. Geotechnical design data in the project area

Soil Class	Unit Weight		Mohr-Coulomb Shear Strength Parameter	
	Total [g/cm ³]	Submerge [g/cm ³]	Cohesion [kg/cm ²]	Angle of Internal Friction [deg]
I	1.9	1	0.2	38
II	1.9	1	0.3	35
III	1.9	1	0.3	30
IV	1.9	1	0.4	27

Note:
For the alternated soil layers, take average values of the geotechnical design data of the soil mass constituent layers.

4. Calculations and comparing to EPB actual result

In this paper face-stabilizing pressures are calculated for excavated stations (N7 and O7) by analytical methods which with EPB actual results are written in the [Table 7](#).

Table 7. Face-stabilizing pressure of analytical methods and EPB shield

Station		N7	O7
Chainage (Km+m)		12+298	13+232
Surcharge(q_s) (KPa)		190	30
Overburden (m)		13.58	22.54
Face-Stabilizing Pressure(σ_T) (KPa)	Attkinson & Patts	56.207	52.803
	Broms	×	×
	Krause	17.589	24.251
	Leca & Dormieux	17.589	15.157
	Carranza-Torres	0.019	×
	Anagnostou & Kovari	×	×
	Broere	78.406	113.062
	Actual result of EPB Shield	81.01	119.95

[Table 7](#) shows the difference between the EPBS actual results and the analytical methods results. As this is clear that conditions of some analytical methods such as Kovari and Broms differ from geotechnical conditions of stations N7 and O7, hence the boxes are filled by putting crosses (×) in the table and if for these stations face-support pressure calculate by them, obtained quantities will be illogical.

5. Prediction of quantity face-stabilizing pressure for some unexcavated stations

The conditions of selected stations differ from together, for example in tunnel depth, cohesion, friction angle, surcharge and etc. Hence different quantities face-stabilizing pressures (σ_T) obtained for these stations by limiting equilibrium analysis method of [Broere](#) which are written in the [Table 8](#).

Table 8. Predicted quantities of face-stabilizing pressure by using Broere method

Station		S7	V7	W7	X7
Chainage (Km+m)		16+757	20+973	22+263	23+743
Overburden (m)		33.35	32.45	9.5	21.25
Surcharge(q_s) (KP)		30	20	40	20
σ_r (KPa)	Method Of Broere	171.676	246.351	25.866	144.532

6. Conclusions

According to the comparison of analytical methods results to EPBS operational results, for this project with these geotechnical properties, limiting equilibrium analysis method of Broere is logical and realistic among others.

It is impossible that all the analytical methods such as Anagnostou and Kovari, Carranza-Torres, Broms and etc use for all parts of Tehran metro line 7 project, because conditions of methods differ together, for example method of Carranza-Torres uses for shallow tunnels and method of Anagnostou and Kovari do not use for cohesive soil.

In Broere method overburden affects on the quantity face-stabilizing pressure more than other parameters like angle of internal friction.

In addition, at the done predictions there are face pressures less than 30 KPa (for the station W7) and more than 230 KPa (for the station V7), so quantity of face-pressure stabilizing depends on project conditions.

References

- [1]. Mohammadi.J, (2010). "Tunnel Face Stability Analysis in Soft Ground by EPB Method(Case Study: Tehran Metro Line 7), M'Sc Thesis, Tehran, Iran.
- [2]. Guglielmetti.V, Grasso.P, Mahtab.A and Xu.Sh, (2007). "Mechanized Tunnelling in Urban Areas, Design Methodology and Construction Control". Geodata S.p.A., Turin, Italy
- [3]. Broere.W, (2001). Tunnel Face Stability & New CPT Applications, Dissertation, TU Delft 2001.
- [4]. Broere.W, (2002). "Influence of excess pore pressures on the stability of the tunnel face". Geotechnical Aspects of Underground Construction in Soft Ground, Toulouse, France.
- [5]. Lece.E & Dormieux.L, (1990). "Upper and lower Bound solutions for the face stability of shallow circular tunnel in frictional", Geotechnique", Vol.40 pp.581-606.
- [6]. Wang.H & Jia.J, (2009). "Face Stability Analysis of Tunnel with Pipe Roof Reinforcement Based on Limit Analysis". EJGE, Vol. 14.
- [7]. Anagnostou.G & Kovari.K, (1993). "Face stability conditions with Earth- Pressure- balanced Shields". Tunneling and Underground Space technology. Vol. 11.No.2.pp.165-173

- [8]. Russo.G, (2003). "Evaluation the required face- support pressure in EPBs advance mode. " Gallerie e Grandi Opere Sotterranee n.71-Dicembre 2003.
- [9]. Jancsecz.S & Steiner.W, (1994). " Face support for large Mix- Shield in heterogeneous ground conditions". Tunneling 94. London.
- [10]. Muller- Kirchenbauer. H, (1972). Stability of slurry trenches Proc, 5th. Europ. Conf . SMFE, Madrid. Vol. I.543-553
- [11]. Carranza- Torres. C, (2004). " Computation of factor of Safety for Shallow Tunnels using Caquot's Lower Bound Solution. " In Publication.
- [12]. Repetto.L, Tuninetti.V, Guglielmetti.V, and Russo.G, (2007). "Shield tunneling in sensitive areas: a new design procedure for optimization of the construction-phase management". GEODATA S.p.A., Torino, Italy.
- [13]. Ribacchi R, (1994). " Recenti orientamenti nella progettazione statica delle gallerie". Atti XVIII Convegno Nazionale di Geotecnica.
- [14]. Anagnostou.G & Rizos.D, (2008). "Geotechnical and contractual aspects of urban tunneling with closed shields". Switzerland.
- [15]. Anagnostou.G & Kovari.K, (1994). " The face stability of slurry- shield driven tunnels", Tunneling and Underground Space Technology, 9(2), 165-174.
- [16]. Kovari, K& Ramoni, M. (2006). Urban tunneling in soft ground using TBMS ". int Conf. & exhibition on tunneling and trenchless technology, Subang Jave- Selangor Darul Ehsan:17-31; the institution of Engineers. Malaysia
- [17]. Anagnostou.G & Kovari.K, (1996). "Face stability in slurry and EPB shield tunneling". Geotechnical Aspects of Underground Construction in Soft Ground, pp. 453–458. Rotterdam, Balkema.
- [18]. W. Broere & van Tol.A.F, (2001). "Time-dependant infiltration and groundwater flow in a face stability analysis". Modern Tunneling Science and Technology, Kyoto, Japan.
- [19]. Chambon.P and Corte. J. F, (1994). "Shallow Tunnels in Cohesionless Soil: Stability of Tunnel Face, Journal of Geotechnical Engineering, ASCE, Vol. 120, No. 7, pp.1148–1165.
- [20]. Muller- Kirchenbaure. H, (1977). Stability of slurry trenches in inhomogeneous subsoil. In. N.N. editor 9th International Conference on Soil Mechanics and Foundation Engineering.
- [21]. Singh.B and Goel. R.K, (1999). Rock Mass Classification, University of Roorkee and Central Mining Research Institute, India.
- [22]. Kim.S.H & Tonon.F, (2010). "Face stability and required support pressure for TBM driven tunnels with ideal face membrane – Drained case". Tunneling and Underground Space Technology.